BMC Cancer

RESEARCH

Open Access

Exploratory analysis of the molecular and genomic landscape of upper tract urothelial carcinoma using long-read sequencing

Zhi Shang[1,2,3†], Xiuxin Ling[4†], Shengming Jin[1,2,3*], Zhenhua Cao[4*], Junlong Wu[1,2,3*] and Dingwei Ye[1,2,3*]

Abstract

Background Upper tract urothelial carcinoma (UTUC), including renal pelvic urothelial carcinoma and ureter urothelial carcinoma, accounts for 10% of urothelial carcinoma (UC). Poorer outcomes and different genetic characteristics of UTUC were reported compared to urothelial carcinoma of the bladder (UCB), which accounts for most cases of UC. Therefore, there is an urgent need for the development of molecular characterization and precision therapies tailored specifically for UTUC.

Methods To elucidate the genetic landscape of UTUC, we included 4 UTUC samples in this study and also perform next-generation sequencing (NGS) of whole exome sequencing. After that, long-read sequencing (LRS) was employed to conduct Whole genome sequencing (WGS) analyses on tumor samples obtained from the four UTUC patients, utilizing the Pacific Biosciences (PacBio) REVIO platform.

Results The clinical phenotypes of four UTUC patients including tumor stage, location and response to treatment, etc. were collected. NGS of four patients yielded negative results. The WGS mapped the mutation landscape in the tumor tissues of four UTUC patients, and screened the sequencing results according to UTUC and solid tumor related genes. Seven pathogenic or likely pathogenic single nucleotide variant (SNV) were obtained. Among the detected structural variations (SVs), four patients shared multiple segments of SVs with close positions. The 12q24.31-p11.1 inversion was shared by four patients. In the detection of STR and DNA methylation, comparing the results of patients and normal controls, many different fragments were obtained. It shows that LRS has important advantages over NGS for accurate tumor detection and treatment.

†Zhi Shang and Xiuxin Ling contributed equally to this work.

*Correspondence:
Shengming Jin
jsmfdu@163.com
Zhenhua Cao
caozhenhua1125@163.com
Junlong Wu
wujunlong920601@163.com
Dingwei Ye
dwye_uro@163.com

Full list of author information is available at the end of the article

Conclusion The analysis revealed multiple genetic variants potentially associated with UTUC carcinogenesis or development, and indicated advantages of TGS over next-generation sequencing (NGS) in cancer genetic variant detection, especially in SV and Short Tandem Repeats (STRs). This study may lay the groundwork for molecular classification and offer valuable insights into the development of precision therapies for UTUC.

Keywords Upper tract urothelial carcinoma, Long-Read sequencing, Molecular and genomic landscape

Introduction

Urothelial carcinoma (UC) is one of the most prevalent malignancies worldwide and can occur anywhere along the urinary tract. While 90–95% of UC cases are located in the bladder (urothelial carcinoma of the bladder, UCB), the development of UC in the upper tract (upper tract urothelial carcinoma, UTUC) is relatively uncommon, accounting for only 5–10% of cases [1, 2]. The systemic management of UTUC has traditionally been based on that of UCB due to the lower incidence of UTUC and limited research. However, emerging data have revealed poorer outcomes and distinct molecular characteristics of UTUC compared to UCB, highlighting the differences in pathogenesis and prognosis between these two diseases as research continues to evolve [3–6]. In particular, UTUC is often invasive at the time of initial diagnosis (60%) compared to UCB(15–25%) [7]. This underscores the importance of understanding the molecular features of UTUC, which may contribute to diagnosis, prognosis, and the development of precision therapies specifically targeting UTUC.

In previous studies, the genomic variations of UC have been explored, with Carlo et al. and Nassar et al. screening for germline pathogenic/likely pathogenic (P/LP) mutations in cancer susceptibility genes and finding that most pathogenic mutations are located in the *BRCA1/2* and *MSH2* genes, although their study cohorts were primarily composed of UCB patients, accounting for over 80% of the cases [8, 9]. Memorial Sloan Kettering Cancer Center (MSKCC) reported that FGFR3 and HRAS alterations are more prevalent in UTUC, while *TP53*, *ERBB2*, and *RB1* mutations are more predominant in UCB [10]. Genomic analyses of UTUC have revealed distinct molecular features compared to UCB. The most commonly identified genomic variations in UTUC patients are single nucleotide variants (SNVs) and small insertions/deletions, detected using next-generation sequencing (NGS). Structural variations (SVs) are present throughout the entire course of the disease and account for 55% of the driver mutations identified in the Pan-Cancer Analysis of Whole Genomes project [11]. The SVs in tumors have been validated as common features and can affect larger regions of the cancer genome than any other type of genetic variation [12].

Long-read sequencing (LRS) technologies developed by Pacific Biosciences (PacBio) and Oxford Nanopore Technologies (ONT) can detect SNVs, SVs, STRs, and even DNA methylation, leveraging their ability to read through repetitive regions with variable GC content [13, 14]. Importantly, LRS achieved significant improvements in throughput and base calling accuracy, currently exceeding 99% [15], making them a remarkable choice for future clinical cancer diagnostics. To date, no study has targeted somatic variations in UTUC using long-read sequencing (LRS).

In the present study, the tumor tissue samples from surgical resection of four UTUC patients in our cohort were collected and used for genetic testing. We use short- and long-read sequencing to obtain a detailed genomic characterization of UTUC patients and compared their efficiency. The molecular evidence for the clinical diagnostic and precision therapy of UTUC are further provided by the sequencing results.

Methods and materials

Patient and sample selection

This study was approved by the Ethics Committee of Fudan University Shanghai Cancer Center (FUSCC), and signed informed consents were obtained from all patients or their corresponding family members. The study included four patients diagnosed with Upper Tract Urothelial Carcinoma (UTUC), specifically including renal pelvic or ureter urothelial carcinoma, as confirmed by histopathology. Patients were eligible if they met the following criteria: (1) histopathologically confirmed diagnosis of UTUC, (2) availability of sufficient high-quality tumor tissue for collection and processing, (3) provision of written informed consent to participate in the study, (4) agreement to have their tumor samples used for next-generation sequencing (NGS) and long-read sequencing (LRS)/whole genome sequencing (WGS) analyses, and (5) the study was conducted in accordance with the Declaration of Helsinki, with approval from the Ethics Committee of Fudan University Shanghai Cancer Center. Tumor samples were collected before chemotherapy for all patients. For the N + patient, sequencing was performed on the primary tumor and not on the metastatic lymph node.

WES

DNA was isolated from tumor samples using the DNA Isolation Kit (Cowin, China) for whole-exome sequencing (WES) via next-generation sequencing. Concentrations were determined on a Qubit fluorometer (Invitrogen,

USA) using Qubit dsDNA HS Assay Kit (Invitrogen, USA). DNA was sheared into 200–300 bp fragments and electrophoresed in a 1% agarose gel to verify the presence of fragments within the desired size range. DNA libraries were prepared using the KAPA Library Preparation Kit (Roche, Switzerland), and purification steps were performed with Agencourt AMPure XP beads (Beckman Coulter, USA). The library concentration was quantified using the Qubit dsDNA HS Assay Kit (Invitrogen, USA), and the DNA library was sequenced on the Illumina NovaSeq platform (Illumina, USA) as paired-end 200-bp reads. After initial variant calling, we applied a multi-step filtering and annotation pipeline to reduce germline variants and sequencing artifacts, since matched normal tissue was not available. Variants were prioritized if they were located in coding or splicing regions, had low population allele frequency, and were supported by pathogenicity databases (ClinVar, HGMD, COSMIC, Mitomap) or in silico prediction scores (SpliceAI, REVEL, Exomiser, VEP). Retained variants were subsequently annotated using VEP (v107). This strategy was adapted from previously validated pipelines, including Wu et al. [16], and provides a reproducible framework for somatic variant analysis in UTUC.

WGS by long-read sequencing

We collected tumor tissue samples from UTUC patients following surgical resection for sequencing. The tissue samples were ground in liquid nitrogen for DNA isolation. Genomic DNA was extracted using the standard phenol-chloroform method. The concentration of extracted DNA was measured using Nanodrop 2000 (Thermo Scientific, USA) and Qubit 3.0 fluorometer (Life Invitrogen, USA). Pulse-field agarose gel electrophoresis was performed using a Bio-Rad CHEF Mapper XA system to assess the integrity, quality, and molecular weight of the DNA. DNA samples were electrophoresed on a 1.0% agarose gel in 0.5x TBE buffer at 14 °C with the following parameters: 6 V/cm, 120°included angle, linear pulse time ramp from 1.0 s to 20.0 s, for 16 h. Approximately 7.5 μg of genomic DNA was fragmented using a g-Tube (Covaris, Australia) with centrifugation at 1600 g. DNA fragments were recovered and prepared for library construction. Rapid purification between steps was performed using SMRTbell cleanup beads (PacBio, USA). The SMRTbell library was constructed using the SMRTbell prep kit 3.0 (PacBio, USA) according to the manufacturer's instructions and sequenced on the PacBio Revio system.

The raw WGS sequencing data were processed using the official software package SMRT Link (version 12.0), as recommended by PacBio, to obtain HiFi reads. Circular Consensus Sequence (CCS) reads were automatically generated by the PacBio SMRT analysis module and mapped to the reference genome GRCh37/hg19 using Pbmm (version 1.10.0). Single-nucleotide variations (SNVs) were called using DeepVariant (version 0.7.0) and annotated with Vep (version 107). Structural variations (SVs) were detected by Sniffles (version 2.0.7) and Cutesv (version 1.0.12), and annotated with AnnotSV (version 3.1.1). STRs were detected using Grandstr (version 1.3.6), developed by Grandomics. DNA methylation analysis was performed with pb-CpG-tools (version 2.3.1) according to the "aligned bam to CpG scores" protocol and annotated with metilene (version 0.2) and AnnotSV (version 3.1.1).

Statistical analysis

All statistical analysis were performed using R software (version 4.4.1), and a significance level of $p < 0.05$ was considered statistically significant. Descriptive statistics were used to summarize patient characteristics, including median age, gender distribution, tumor stage, and treatment regimens. Continuous variables were presented as medians with ranges, while categorical variables were expressed as counts and percentages. For survival analysis, Kaplan-Meier curves were generated to assess the association between genetic alterations and patient outcomes, and differences between groups were evaluated using the log-rank test.

Results

Study design

The cohort comprised four patients (2 males and 2 females) with a median age of 64.5 years (ranging from 60 to 70 years). Tumor samples were collected from all four UTUC patients at Fudan University Shanghai Cancer Center and processed for LRS (Fig. 1A). The study was conducted in accordance with the Declaration of Helsinki. Informed consent was obtained from all enrolled patients, and the study was approved by the Ethics Committee of Fudan University Shanghai Cancer Center (2008222-22).

Clinical features

A total of four UTUC patients were analyzed in this study, and their baseline characteristics are summarized in Table 1. The median age at diagnosis was 65 years (range, 60 to 70 years), with an equal gender distribution (50% male). In terms of laterality, two patients (50%) were left and two patients (50%) were right. One patient was classified as pT1, and three patients (75%) were classified as pT2-pT3. The first patient underwent transurethral resection of bladder tumor (TURBT) and left radical resection of ureteral cancer; the second patient underwent right radical nephrectomy; the third underwent right hemi-urectomy; and the fourth underwent left hemi-urinary tract radical resection. Histopathological

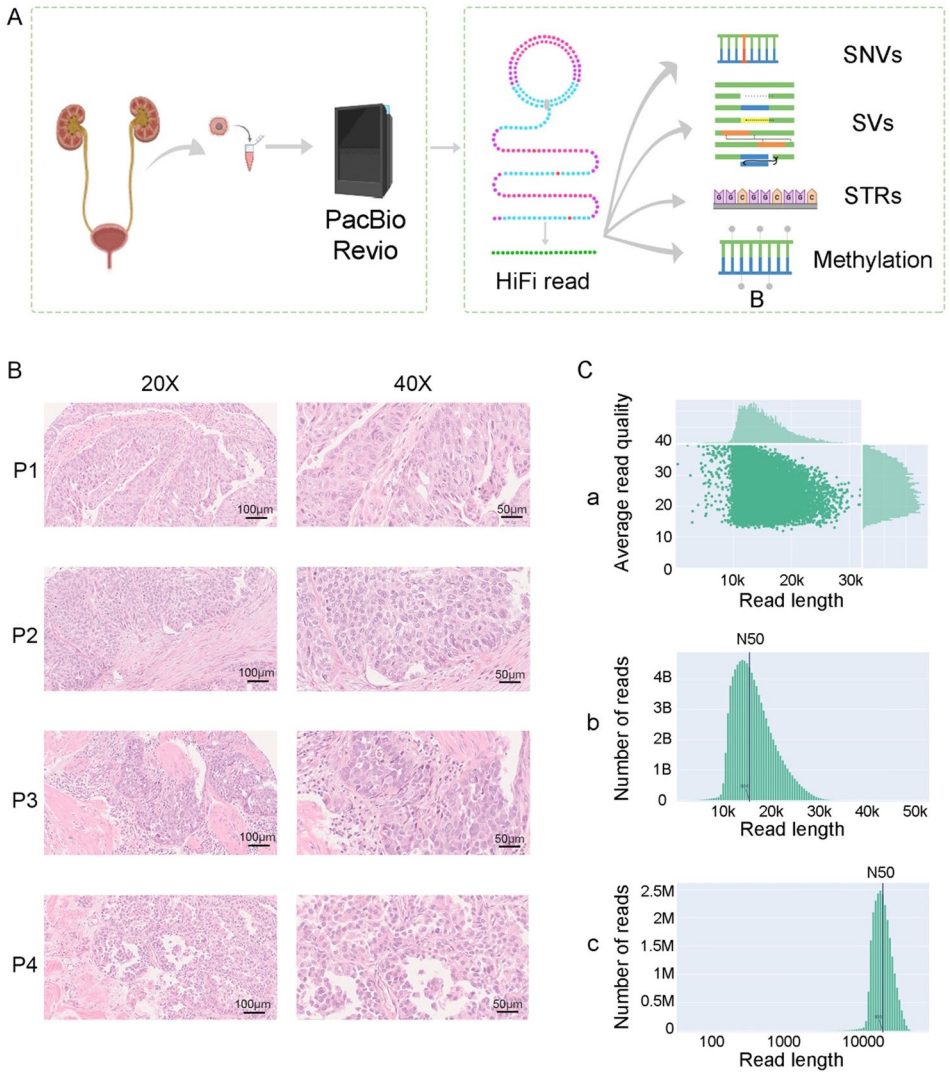

Fig. 1 Long-read sequencing study design and histopathological analysis. **A** Flowchart of the study design. **B** Histopathological analysis of four high-grade patients with UTUC. **C** Sequencing data quality assessment. **a** Plot of read lengths versus average read quality. **b** Weighted histogram of read lengths; (**c**) Weighted histogram of read lengths after log transformation

examination confirmed invasive high-grade urothelial carcinoma in all four cases (Fig. 1B). Post-surgery, all patients received chemotherapy: two were treated with the GC regimen, and two with the GP regimen.

Sequencing data analysis

Tumor samples were subjected to WES using the Illumina NovaSeq platform. Copy number variant(CNV), single nucleotide variation (SNV), and small insertions/deletions (indel) were analyzed and reported. Variant statistics detected by NGS with paired-end 150 bp short reads are summarized in Table S1. Data from the WES of four tumor samples were analyzed, but no disease-associated SVs were identified. As a result, we proceeded with additional sequencing using long-read technology for further analysis.

The four tumor samples were subjected to PacBio WGS, generating high-quality WGS datasets for the present study (Fig. 1C). On average, we obtained 88.82 Gb of clean data per sample, with a median read length of 14.71 kb from PacBio long-reads after quality control. The average coverage of the target region across all four samples was 99.47%. The dataset had an average depth of 31X, with an average of 6043478.25 reads per sample. Detailed data for each sample are provided in Table S2. To comprehensively explore the genetic basis of UTUC, we characterized the full spectrum of genetic alterations, including CNVs, SNVs, SVs, STRs, and DNA methylation across the whole genome or exome.

Table 1 Clinical features of four patients

Case	Age	Sex	Laterality	Location	T stage	N stage	M stage	Pathologic grade	Carcinoma in situ	UCB cancer history	Non-UCB cancer history	Chemotherapy	Treatment effect
P1	64	Female	Right	Both	T2	0	0	High	No	Yes	No	GP	Resistant
P2	64	Female	Right	Renal pelvis	T1	0	0	Low	No	No	Yes	GC	Sensitive
P3	70	Male	Left	Ureter	T3	0	0	High	Yes	No	No	GC	Intermediate
P4	60	Male	Left	Ureter	T2	2	0	High	No	Yes	No	GP	Resistant

The T stage in this table refers to the pathological grading of tumor size and extent based on the TNM classification system

Landscape of genomic alterations in UTUC tumor samples

Based on the LRS data from four tumor samples, we constructed the landscape of genomic alterations. P1 and P4 exhibited marked chromosomal instability (CIN), characterized by large-scale copy number variations (CNVs) and widespread allelic imbalance (AI) regions (Fig. 2A). Most AI regions coincided with copy number alterations (Fig. 2B), consistent with LOH or copy number-dependent allelic imbalance.

SNVs

During the processing of the LRS data, SNVs were called and quality-controlled for analysis. Genes frequently mutated or commonly altered in UTUC or other solid cancers, as reported by the COSMIC and OncoKB databases, were analyzed. A complete list of these genes is provided in Table S3. Subsequently, mutation types, including frameshift, nonsense, splice-3/5, stop-gain, and init-loss variants, were further screened and analyzed. We detected a total of 2,579,270 small mutations, including SNVs/InDels, across the four tumor samples, with an average of 644,817 variants per sample. After filtering, 43,151 mutations were identified, with an average of 10,787 mutations per sample. Among all the tumor samples, missense mutations (64%) and splice mutations (15%) were the two most common SNVs classifications. The SNVs classifications for each patient are shown in Fig. 3A-B. Subsequently, we further filtered mutations in UTUC and solid cancer related genes, resulting in 264 remaining mutations (Table S4). The six most frequently altered UTUC and solid cancer related genes are *RET* (37, 14.34%), *HRAS* (23, 8.91%), *BRCA1* (19, 7.36%), *BRCA2* (19 mutations, 7.36%), *NRG1* (13, 5.03%), and *KRAS* (12, 4.65%) (Fig. 3E). Next, we screened for frameshift, nonsense, splice-3/5, stop-gain, and init-loss variants mutations in these UTUC and solid cancer related genes. A total of 13 mutations in *BRAF*, *BRCA2*, *CREBBP*, *KMT2A*, *KMT2D*, *PTEN*, and *TP53* are summarized in Table 2. After screening for pathogenicity and relevance to UTUC, the most common SNV identified in the four samples were in *KMT2D* (4/13, 30.77%) and *PTEN* (4/13, 30.77%). Three mutations were classified as pathogenic according to the American College of Medical Genetics and Genomics (ACMG) guidelines: *KMT2A* c.2318del p.Pro773ArgfsTer8 (P1), TP53 c.994-1G>C (P3), and *BRCA2* c.793+1G>T (P2). Additionally, three mutations in *KMT2D*, including c.4584-7_4595del, c.16,329 C>G, and c.11,812 C>T, were classified as likely pathogenic. The frameshift mutation *PTEN* c.154+1del was present in all four samples, suggesting it may be a hotspot mutation in UTUC tumor samples.

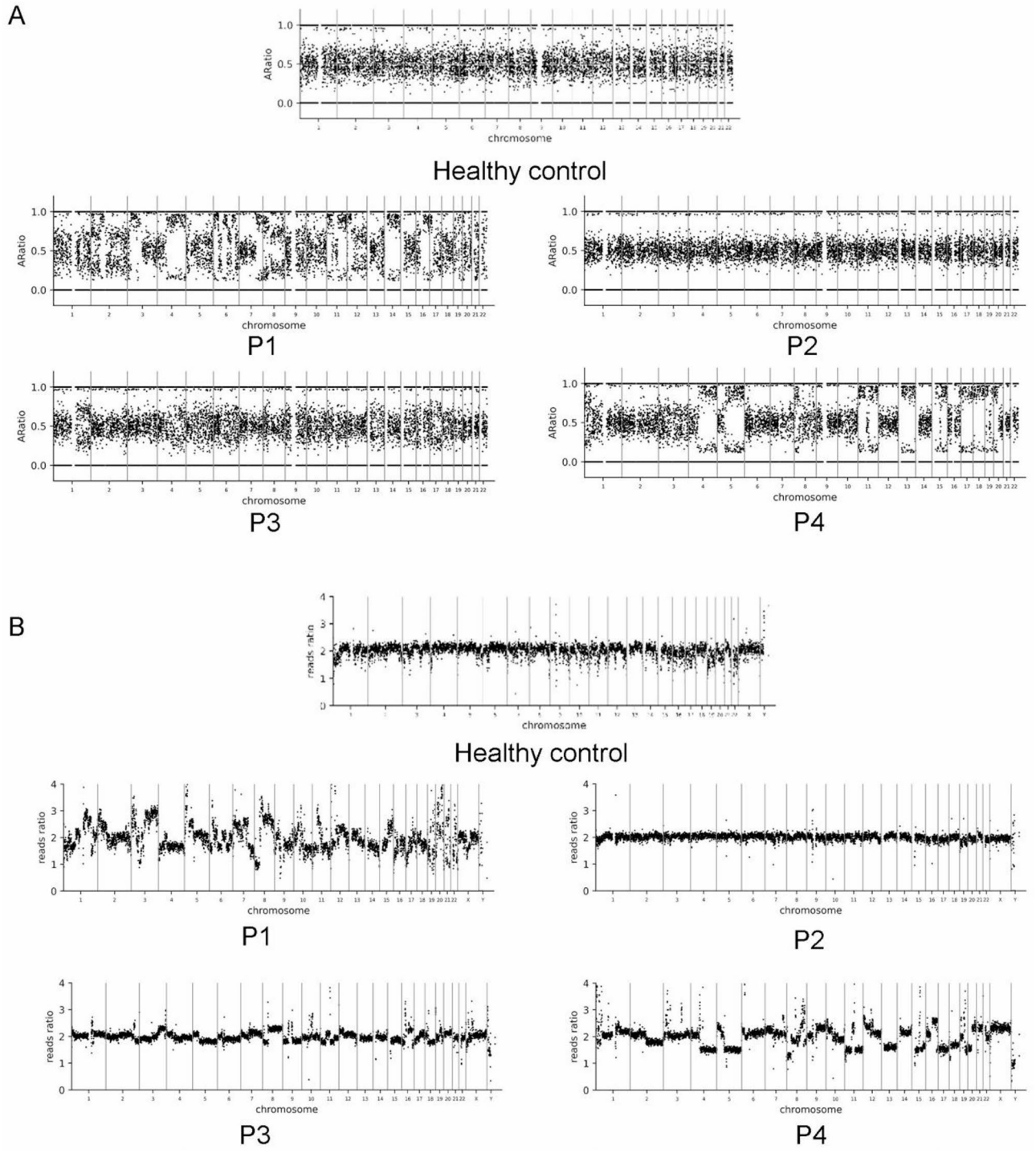

Fig. 2 The genomic landscape of four patients with UTUC. **A** Uniparental Disomy (UPD) Analysis: Distribution of UPD events across each chromosome in four UTUC patients compared to healthy controls. **B** Copy Number Variation (CNV) Analysis: Overview of CNV profiles in four UTUC patients compared to healthy controls

SVs

Based on long-read sequencing WGS data from four tumor samples, a total of 18,510 SVs were identified, with an average of 4627 SVs per sample. Of all the SVs detected in WGS, deletions (Del) and insertions (Ins) were the two most frequently observed SV variation classifications, accounting for 46% and 44% of the total SVs, respectively (Fig. 3C-D). SVs were categorized by size into < 100 bp, 100 bp–1 kb, 1–10 kb, and > 10 kb. Among these categories, SVs < 100 bp (39%) and SVs 100 bp–1 kb (48%)

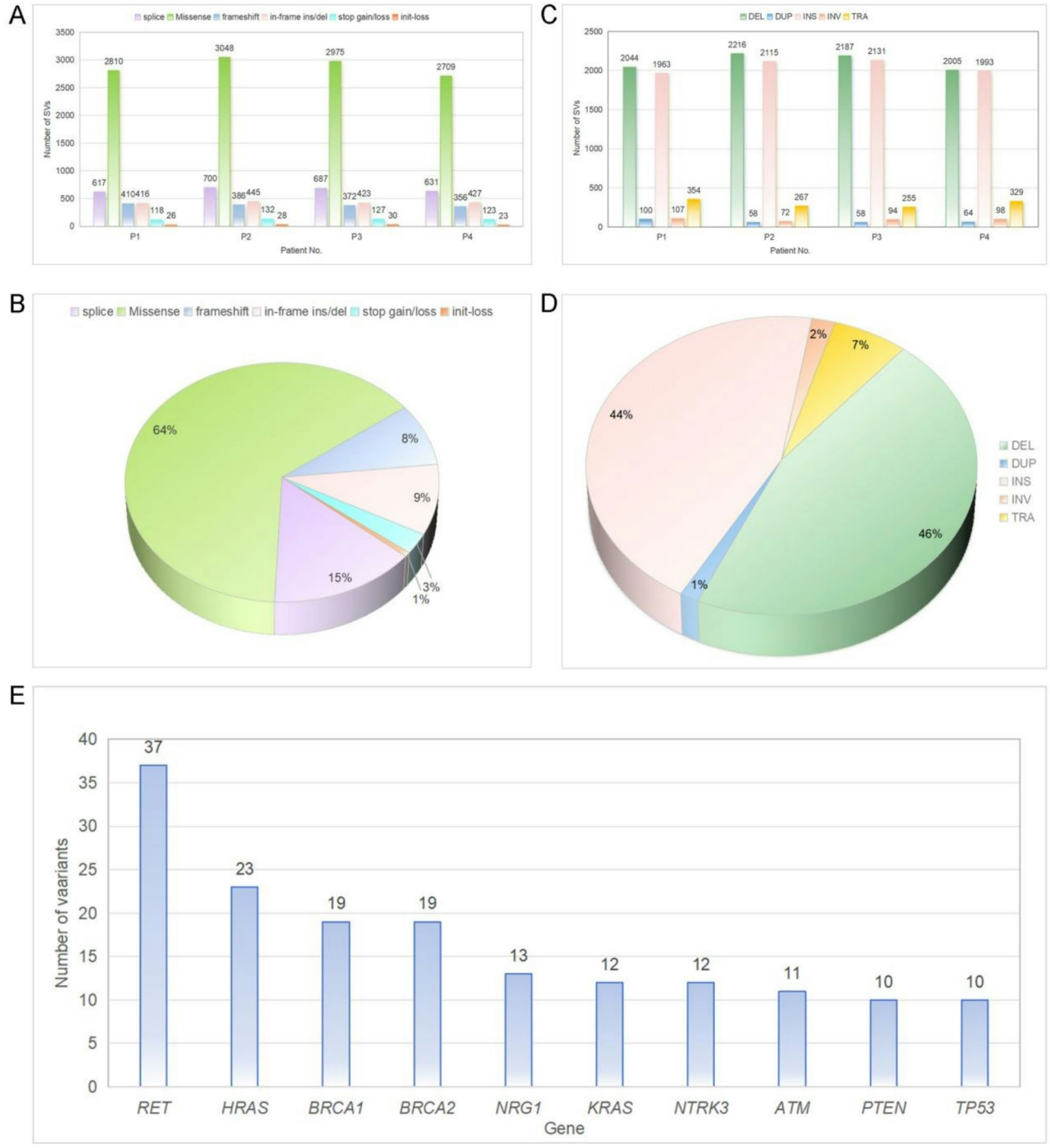

Fig. 3 The SNVs and SVs identified by LRS in four patients with UTUC. **A** Classification of SNVs detected in four patients. **B** Overall classification of SNVs detected in the four patients. **C** Classification of SVs detected in four patients. **D** Overall classification of SVs detected in the four patients. **E** Frequency of SNVs involving tumor associated genes after screening in four patients

constituted the majority of the detected SVs (Fig. 4A). The distribution of SV counts across individual samples was consistent with the overall results. Chromosome 1 (Chr 1) had the highest number of SV breakpoints, followed by Chr 7 and Chr 2 (Fig. 4B). The SVs in the four samples were screened based on a gene list associated with UTUC and solid tumors, resulting in 24, 15, 15, and 25 SVs, respectively. Detailed information on the filtered SVs was presented in Table S5. Notably, the breakpoints of the filtered SVs were most frequently located on chromosome 7, specifically within the 7q36.1 region. Based on these results, the common SVs among the four samples

Table 2 Screened SNVs identified by WGS

Sample ID	#Chrom	Position	Start position	Stop position	Zygosity	Transcript	Gene	cHGVS	pHGVS	Mutation type	HGMD classification	Evidence
P1	chr10	intron1	89623861	89623861	Hom	NM_001304717.5	*PTEN*	c.154+1del			benign	BA1+BP7
P1	chr11	exon3	118344186	118344186	Het	NM_001197104.2	*KMT2A*	c.2318del	p.Pro773ArgfsTer8	frameshift	pathogenic	PVS1+PM2_supporting+PS2
P1	chr12	exon18	49439946	49439964	Het	NM_003482.4	*KMT2D*	c.4584-7_4595del		splice-3	likely pathogenic	PVS1+PM2_supporting
P1	chr16	exon31	3778440	3778464	Het	NM_004380.3	*CREBBP*	c.6584_6608del	p.Arg2195AsnfsTer99	frameshift	likely pathogenic	PVS1+PM2_supporting
P1	chr7	exon10	140482927	140482927	Het	NM_004333.6	*BRAF*	c.1208del	p.Pro403LeufsTer8	frameshift	VUS	PVS1_Moderate+PM2_supporting
P2	chr10	intron1	89623861	89623861	Hom	NM_001304717.5	*PTEN*	c.154+1del			benign	BA1+BP7
P2	chr13	intron9	32905168	32905168	Het	NM_000059.4	*BRCA2*	c.793+1G>T		splice-5	Pathogenic	PVS1+PS4_Moderate+PM2_supporting
P3	chr10	intron1	89623861	89623861	Hom	NM_001304717.5	*PTEN*	c.154+1del			benign	BA1+BP7
P3	chr12	exon52	49416382	49416382	Het	NM_003482.4	*KMT2D*	c.16329C>G	p.Tyr5443Ter	stop-gain	likely pathogenic	PVS1+PM2_supporting
P3	chr17	intron9	7574034	7574034	Het	NM_000546.6	*TP53*	c.994-1G>C		splice-3	Pathogenic	PVS1+PS4_Moderate+PM2_supporting
P4	chr10	intron1	89623861	89623861	Hom	NM_001304717.5	*PTEN*	c.154+1del			benign	BA1+BP7
P4	chr12	exon40	49426676	49426676	Het	NM_003482.4	*KMT2D*	c.11812C>T	p.Gln3938Ter	stop-gain	likely pathogenic	PVS1+PM2_supporting
P4	chr12	exon15	49441851	49441876	Het	NM_003482.4	*KMT2D*	c.4132-24_4133del		splice-3	VUS	PVS1_Strong+PM2_supporting

Hom Homozygous, *Het* Heterozygous, *VUS* Variant of Uncertain Significance

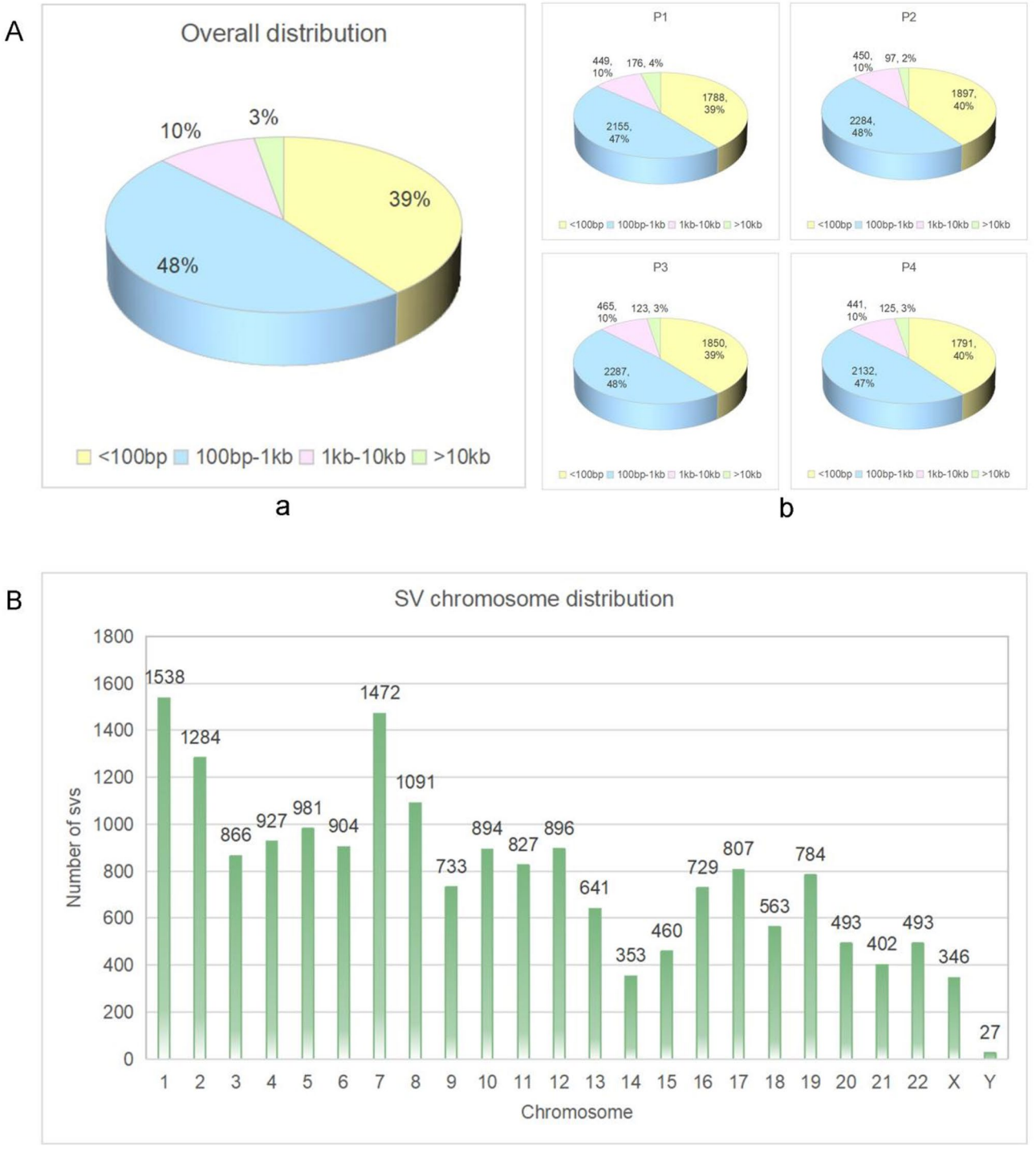

Fig. 4 Length of structural variation and chromosome distribution in four patients with UTUC. **A** Distribution of SVs detected in different length intervals (**a**) Percentage of structural variants detected in different length intervals (four patients) (**b**) Distribution of SVs detected in different length intervals among patients P1-P4. **B** Chromosomal Distribution of SVs: Number of SVs per chromosome in four patients

were compared and summarized in Supplementary Material 3. The structural variations shared by the four samples include a 2q22.1 deletion (covering the *LRP1B* gene), a 10q26.13 insertion (covering the *FGFR2* gene), a 12q24.31-p11.1 inversion (covering the *MDM2* gene), a 13q14.2 insertion/deletion (covering the *LPAR6* and *RB1* genes), and a 17q12 deletion (covering the *CDK12* gene). Among these SVs, the 12q24.31-p11.1 inversion has the same start (chr12:25956127) and end (chr12:125801148) coordinates across all samples, suggesting that this SV

may represent a hot spot mutation site in UTUC tumor tissues.

Short tandem repeat and DNA methylation

A total of 64 known pathogenic STRs were analyzed based on the LRS results. STRs with repeat counts outside the normal range are listed in Table 3. Bar plots illustrating the repeat counts of these STRs are shown in Figure S1. STR fragments with abnormal amplification and their corresponding repeat counts for each patient are summarized in Fig. 5A. The genes involved in repeat expansion fragments include *XYLT1*, *NIPA1*, *POLG*, and *AFF2*. In addition to genomic variations, abnormal DNA methylation (DNAme), particularly focal hypermethylation at tumor suppressor genes (TSGs) promoters, contributes to the inactivation of these genes, thereby promoting cancer development. Differentially methylated regions (DMRs) between haplotypes 1 and 2 were identified and analyzed, with the results presented in Table 4. The overall DNAme profiles for patients P1 to P4 are depicted in Fig. 6.

Discussion

The most common presenting symptom of UTUC is hematuria, which can be either grossly visible or microscopically detected, while flank pain and other urinary symptoms may also occur but are less specific [17]. Diagnosis typically relies on a combination of imaging modalities, such as computed tomography urography (CTU), retrograde pyelography, and ureteroscopy with biopsy or cytology. However, the accuracy of biopsy can be limited by factors such as small sample size and crush artifacts [17, 18]. Radical nephroureterectomy remains the gold standard treatment for localized UTUC, involving the removal of the affected kidney, the entire ureter, and a cuff of the bladder. In selected cases, kidney-sparing endoscopic procedures, such as ureteroscopic resection or laser ablation, may be considered for low-risk, non-invasive tumors or for patients with comorbidities that preclude major surgery [17, 19]. In our cohort, two patients (P1 and P4) had a history of bladder cancer, while P2 and a first-degree relative had a history of non-bladder cancer. According to our results, P1 and P4 carry large-scale copy number variations (CNVs) and widespread allelic imbalance (AI) regions. Additionally, P1 and P4 exhibited drug resistance during treatment. These phenomena may be associated with their history of bladder cancer. Their drug resistance might also be related to the high level of UPD detected.

According to previous research, factors influencing prognosis include tumor grade (high-grade tumors are more aggressive), the presence of lymph node metastasis, and specific genetic alterations. UTUC exhibits a distinct spectrum of genetic alterations compared to UCB. In UCB, frequent genomic alterations primarily occur in the RTK-Ras-PI3K pathway (including *FGFR3*, *HRAS*, *PIK3CA*, and *ERBB2*), the p53-Rb pathway (including *TP53*, *RB1*, *CCND1*, and *CDKN2A*), and chromatin modifiers (including *KMT2D*, *KMT2C*, *KDM6A*, and *CREBBP*) [20–23]. In contrast, *FGFR3* mutations, which are common in UTUC, particularly in low-grade, non-muscle-invasive tumors, lead to constitutive activation of receptor tyrosine kinase, promoting cell proliferation. Conversely, *TP53* mutations are associated with a more aggressive phenotype and poorer prognosis. Genetic variations at specific loci, such as the T allele of rs9642880 on chromosome 8q24, have been shown to confer an increased risk of developing UTUC and are also associated with tumor aggressiveness [24]. In addition, tumors with *FGFR3* alterations may have a relatively better prognosis compared to those with *TP53* alterations [18, 24, 25]. As TP53 mutations as a key driver of aggressive phenotypes in bladder cancer, particularly within the basal-squamous subtype, where they contribute to enhanced tumor invasiveness and adverse clinical outcomes [23].

We used a list of UTUC and solid tumor related genes to screen the SNVs identified in LRS and 264 mutations are screened out. The top three frequently occured SNV in our cohort including *RET* (37, 14.34%), *HRAS* (23, 8.91%), *BRCA1* (19, 7.36%), and *BRCA2* (19, 7.36%). *RET* gene alterations have been reported related to thyroid cancer and small-cell lung cancer (SCLC) by activating the ERK signaling and changing the MYC expression, thus increasing cell proliferation to aid the development of the cancer. The *RET* mutations identified provides a new sight into the relationship between *RET* gene and UTUC which should be valid in a larger cohort. Seven mutations appeared in these genes are classified as pathogenic/likely pathogenic, including the mutations in gene *KMT2A*, *KMT2D*, *CREBBP*, *BRCA2*, *and TP53*. The genes with the most P or LP mutations are the *KMT2D* gene. Fujii et al. sequenced 199 tumor sample from UTUC patients, the results show that the *TP53* and *CCND1* were more commonly affected in invasive UTUC, whereas *FGFR3*, *HRAS*, and the *TERT* promoter mutations were more frequent in non-invasive UTUC. Frequencies of genetic variations were also related to the location of tumors samples used for sequencing. ureter cancers showed notably higher frequencies of *KMT2D* and *TP53* mutations, whereas *HRAS*, *KDM6A*, and the TERT promoter were more commonly mutated in pelvic tumors [5]. Only P2's tumor located in renal pelvis. Her top three frequently appeared mutated genes are *BRCA1*, *HRAS*, and *RET*. The highly appearance of *HRAS* genes mutations in P2 are consistent with Fujii's research. The *RET* gene and *HRAS* gene belongs to proto oncogene, which are mainly responsible for regulating the processes

Table 3 Filtered Abnormally amplified STR fragments identified by WGS

Patient ID	Chromosome	Start position	End position	Ref_gene	Ref_func	Motif	Normal range	Pathogenic range	Genetic_mode	Allele1 repeat number	Allele2 repeat number	Max repeat number	Repeat_Stat
P1	16	17564765	17564779	*XYLT1*	UTR5	GCC	9~20	≥72	AR	31	31	32	30:1,31:15,32:1
P1	15	23086364	23086402	*NIPA1*	exonic	CGC	8	≥10000	AD	11	12	13	11:8,12:8,13:1
P1	15	89876806	89876859	*POLG*	exonic	CTG	≤15	10000	AD/AR	17	17	18	16:1,17:27,18:1
P1	6	45390488	45390538	*RUNX2*	exonic	GCR	17	20~27	AD	16	16	18	15:1,16:16,17:1,18:1
P1	X	147582056	147582330	*AFF2*	UTR5	CCG	4~39	≥200	XLR	80	79	81	71:1,79:5,80:21,81:3
P2	16	17564765	17564779	*XYLT1*	UTR5	GCC	9~20	≥72	AR	31	31	32	7:1,30:2,31:18,32:1
P2	4	39350045	39350103	*RFC1*	intronic	AAGGG	0~99	≥100	AR	12	12	141	11:1,12:5,141:1
P2	3	183429951	183430016	*YEATS2*	intronic	TTTCA	12	192	AD	10	42	43	10:15,42:15,43:1
P2	15	23086364	23086402	*NIPA1*	exonic	CGC	8	≥10000	AD	11	11	12	11:20,12:2
P2	15	89876806	89876859	*POLG*	exonic	CTG	≤15	10000	AD/AR	17	17	18	16:2,17:28,18:2
P2	4	160263679	160263768	*RAPGEF2*	intronic	TTTCA	18	18	AD	18	17	19	16:1,17:13,18:15,19:1
P2	X	25031767	25031814	*ARX*	exonic	GCR	10~16	17~27	XL	15	15	17	14:1,15:18,16:1,17:1
P2	X	147582056	147582330	*AFF2*	UTR5	CCG	4~39	≥200	XLR	79	83	85	68:1,76:1,78:1,79:9,81:1,82:4,83:7,85:2
P3	16	17564765	17564779	*XYLT1*	UTR5	GCC	9~20	≥72	AR	31	30	32	29:1,30:9,31:10,32:1
P3	3	183429951	183430016	*YEATS2*	intronic	TTTCA	12	192	AD	39	10	40	10:16,39:26,40:1
P3	13	70713516	70713561	*ATXN8OS*	exonic	CTG	15~50	54~250	AD	17	65	67	16:3,17:10,18:1,63:1,64:1,65:3,66:2,67:2
P3	14	23790681	23790711	*PABPN1*	exonic	GGC	10	11~18	AD	10	10	11	8:1,9:1,10:25,11:1
P3	15	23086364	23086402	*NIPA1*	exonic	CGC	8	≥10000	AD	12	12	14	11:1,12:27,13:4,14:1
P3	15	89876806	89876859	*POLG*	exonic	CTG	≤15	10000	AD/AR	17	17	18	17:24,18:2
P3	8	119379055	119379158	*SAMD12*	intronic	TTTCA	21	≥105	AD	21	19	22	17:2,18:1,19:21,20:5,21:22,22:1
P3	X	25031767	25031814	*ARX*	exonic	GCR	10~16	17~27	XL	15	15	18	15:14,18:1
P3	X	147582056	147582330	*AFF2*	UTR5	CCG	4~39	≥200	XLR	80	80	80	78:1,79:1,80:16
P4	16	17564765	17564779	*XYLT1*	UTR5	GCC	9~20	≥72	AR	30	4	30	4:3,16:1,29:2,30:23
P4	15	23086364	23086402	*NIPA1*	exonic	CGC	8	≥10000	AD	12	12	13	11:1,12:19,13:1
P4	15	89876806	89876859	*POLG*	exonic	CTG	≤15	10000	AD/AR	17	17	18	17:26,18:2
P4	4	160263679	160263768	*RAPGEF2*	intronic	TTTCA	18	18	AD	20	20	21	19:1,20:13,21:1
P4	8	119379055	119379158	*SAMD12*	intronic	TTTCA	21	≥105	AD	18	17	24	17:7,18:34,19:2,23:1,24:1
P4	X	147582056	147582330	*AFF2*	UTR5	CCG	4~39	≥200	XLR	82	81	83	79:1,80:1,81:6,82:9,83:2

AD Autosomal Dominant, *AR* Autosomal Recessive, *XLR* X-Linked Recessive

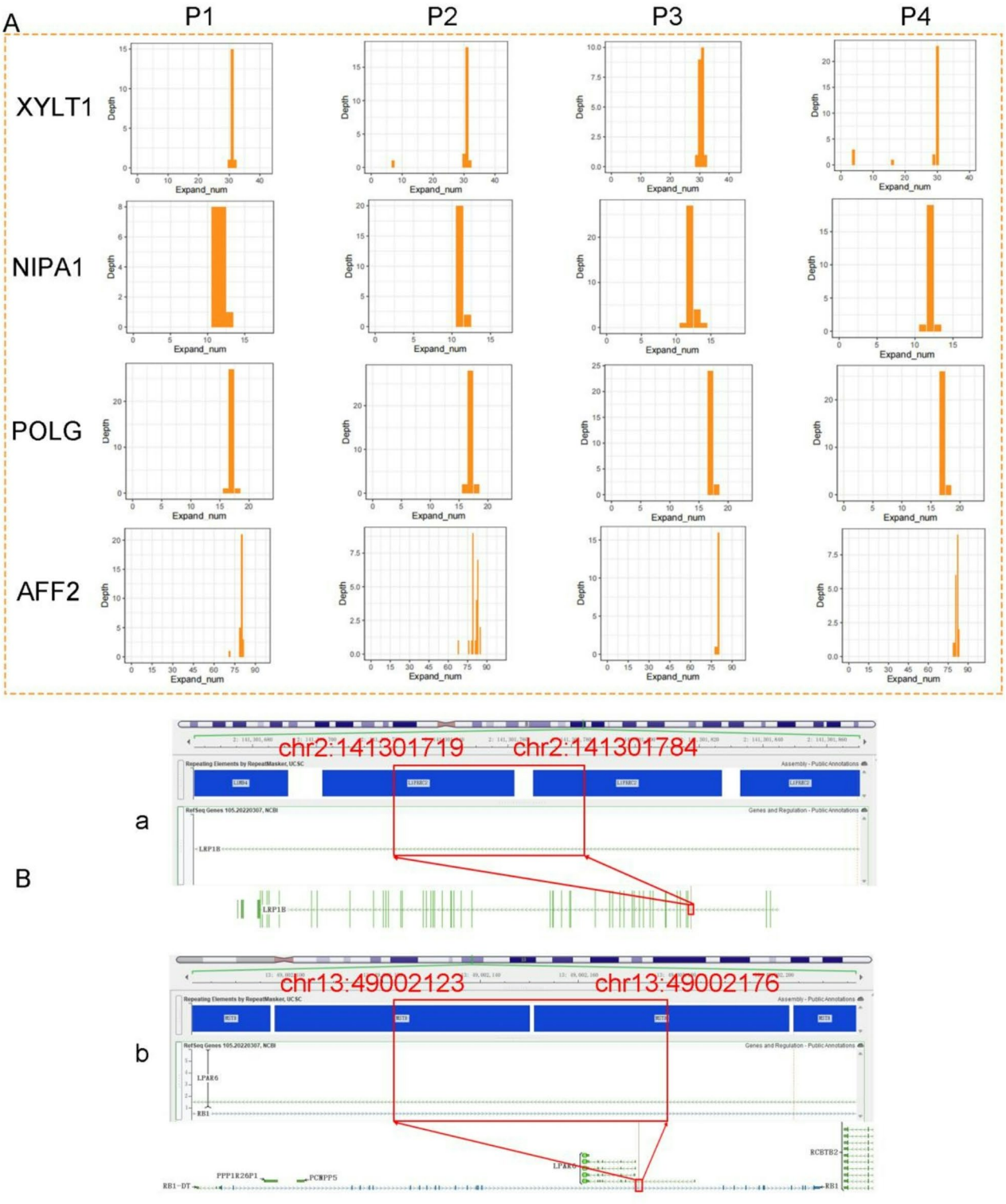

Fig. 5 STR detection in four patients with UTUC. **A** Histogram of abnormal repeat expansions: Frequency of abnormal repeat expansions in the same gene detected across all four patients. **B** Examples of schematic of deletions identified in patients: (**a**) Schematic of deletion mutation in *LRP1B* Gene (P1). **b** Schematic of deletion mutation in *LPAR6* and *RB1* genes (P1)

Table 4 DMRs identified in four patients by WGS

Patient ID	Tested methylation sites	DMR
P1	27573237	216832
P2	27826746	247302
P3	27982849	290793
P4	27936874	197186

DMR Differentially Methylated Region

of cell growth, proliferation, and differentiation. Whereas the *BRCA1/2* genes belongs to Homologous recombination repair (HR) pathway. In another research of 309 Chinese cohort, the most frequently mutated genes were *MSH2* (10/309, 3.2%); *BRCA2* (10/309, 3.2%); *BRCA1* (4/309, 1.3%); and *BRIP1* (3/309, 1%) [16]. The reason

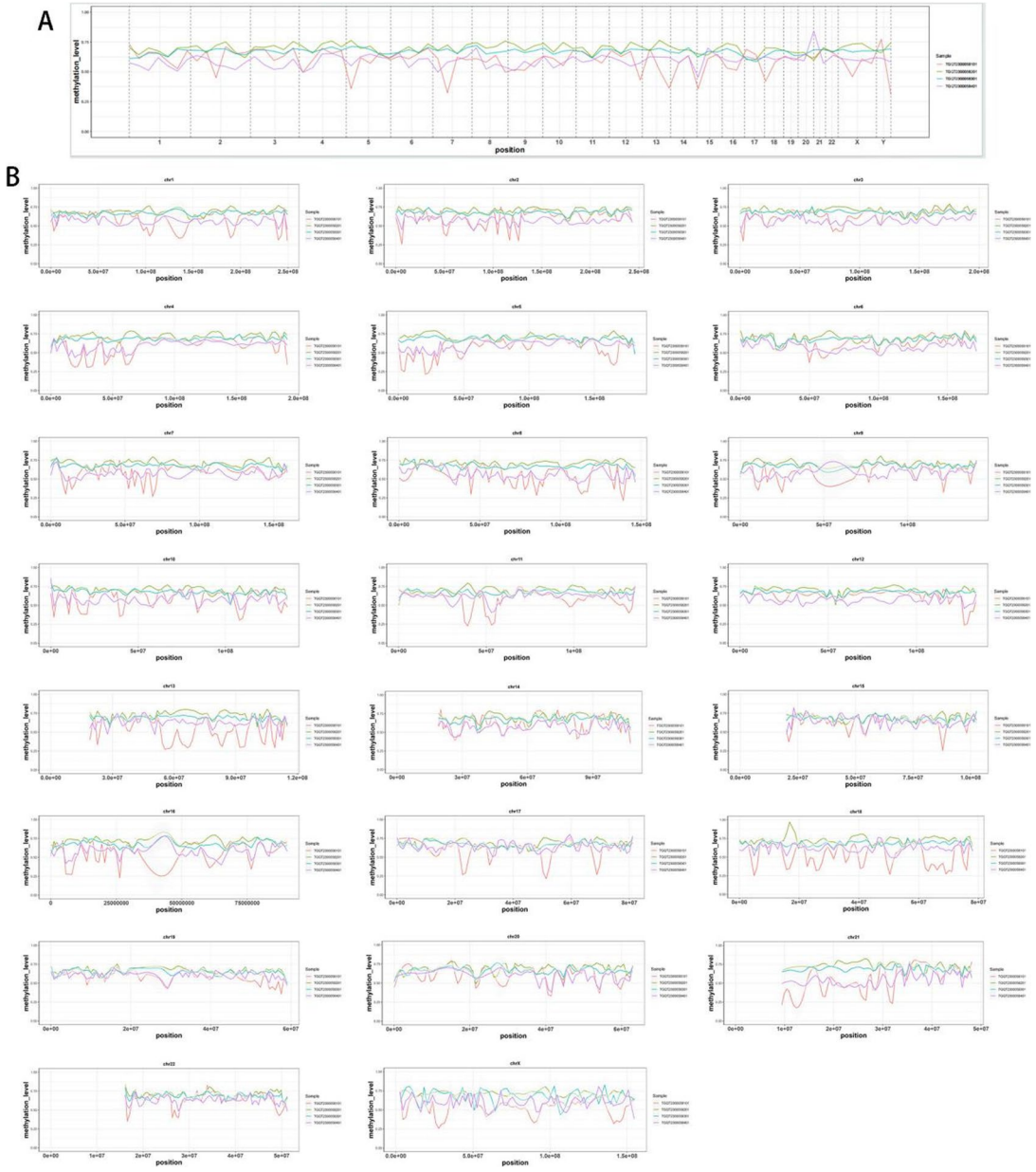

Fig. 6 DNA methylation of the genomic of four patients with UTUC. **A** Overall methylation of four patients. **B** Methylation of each chromosome in four patients

that the frequencies of the mutated genes are different with the previous research may due to the limited samples of our research. However, the frequent mutations in our research may provide new insight of the genomic mutation landscape of the UTUC tumor tissue.

The SVs identified in our research contribute to the large fragment variations in UTUC, since the LRS are suitable and advantageous in SVs testing. The previous research about the SVs in UTUC are limited. 17p13 deletions including TP53 and other genes represent a common cause for reduced/lost p53 function in tumor cells and are linked to tumor aggressiveness [18, 24, 25]. Duy D. Nguyen et al. researched the chemotherapy-induced mutations within extrachromosomal DNA (ecDNA)-forming SVs and found that most CCND1 amplifications in UC arise within circular ecDNA-forming SVs. EcDNA forming SVs increased in complexity and contributed to the evolution of treatment resistance [26]. In our cohort, we analyzed the LRS WGS results target UTUC tumor tissues and identified a SV that was appear in four patients in 12q24.31-p11.1 (chr12: 25956127–125801148). At present, inv [12] has been reported to be associated with vulvar leiomyoma and malignant hematologic malignancies [27, 28]. However, other research also reported that pericentric inv [12](p12.3q14) does not affect phenotype [29]. At present, there is no research report on the correlation between inv [12] and UTUC. However, all of our patients carried the same inversion in their tumor tissue, which is the preliminary indication of the correlation between inv [12] and UTUC. However, these should be explored and verified in larger sample. The inv [12] covered the cancer related genes including *KMT2D* and *MDM2*, which may affect the function of these two genes, resulting in the occurrence of tumors. Because the variations of the above two genes have been reported many times in UTUC genomic variations [5]. We also identified 8 deletions in 2q22, covering *LRP1B* gene; 7 deletions in 17q12, covering *CDK12* gene; 4 insertions in 10q26.13 covering *FGFR2* gene, and 2 deletion and 3 insertions covering *LPAR6* and *RB1* gene. Although the starting and ending chromosomal positions of the above structural variations are different, they cover the same gene. Deletion or insertion of the same gene may have the same effect. Among the genes included in the above SVs, *RB1* and *LRP1B* genes have been reported to be related with UTUC [23]. In our research, we identified the breakpoints of the structural variation (SV) del(2q22.1) in four patients (P1: chr2: 141301719–141301784, P2: chr2: 141301716–141301781, P3: chr2: 141301719–141301783, P4: chr2: 141301718–141301783). These breakpoints are located within the Long Interspersed Nuclear Elements (LINEs) L1PREC2 shown in Fig. 5B (a). Previous studies have shown that the expression of LINE-1 is associated with tumorigenesis in several cancers [29]. Another SV identified in Patient 1 (P1) may be correlated with upper tract urothelial carcinoma (UTUC) shown in Fig. 5B (b). The breakpoints of this SV are chr13:49002123 and chr13:49002176, which are located within both the LPAR6 and RB1 genes. Notably, loss of 13q14.2 has been reported as one of the most common copy number variations (CNVs) in chronic lymphocytic leukemia (CLL) [30–32].

In breast cancer, mutations or loss of single genes within the 13q14.2 region, such as Retinoblastoma 1 (RB1) [33, 34], have also been associated with the disease. This loss is widespread across various cancers, with the highest frequencies observed in testicular cancer (75%), kidney cancer (67%), and squamous cell lung cancer (66%) [30–32]. To date, the relationship between this SV and UTUC has not been extensively studied. Our study preliminarily demonstrates a correlation between the two. However, since this SV spans two genes-LPAR6 and RB1-further investigation is needed to elucidate the mechanisms by which this SV contributes to UTUC pathogenesis. Exploring the relationship between these genes and UTUC may uncover new targets for the management and treatment of this disease [30–32].

STR has been shown to be associated with a variety of diseases, especially neurological and neurodegenerative disorders. The abnormalities of STR are rarely explored in other diseases.The limitation of sequencing technology is one of the limiting factors. Graham S et al., found 160 recurrent repeat expansions enrichment near candidate cis-regulatory elements using LRS. A GAAA-repeat expansion was identified in 34% of renal cell carcinoma samples nearing a regulatory element in the first intron of UGT2B7 [35]. That suggesting the necessary of STR detection in cancer samples and the superiority and reliability of LRS in detecting STR fragments. Four STRs in genes *XYLT1*, *NIPA1*, *POLG*, and *AFF2* were identified among all of our patients. Gene *XYLT1*, *NIPA1*, and *POLG* have been related to multiple inherited disease [36–38]. AFF2 gene fusion has been demonstrated that was associated papillary squamous cell carcinoma of the sinonasal tract [39]. However, the relationship among these STRs with UTUC still needed to be verified in larger cohort. Their pathogenicity and the specific pathogenic repeat number range of these STRs also need to be explored in combination with functional experiments. However, our experiment shows the preliminary correlation between STR fragments and UTUC, and also shows the new application scope of LRS in the precise diagnosis of tumors. The sample size limits the generalizability and interpretability of the genetic findings. While this study demonstrates the feasibility of using LRS on UTUC samples and generates preliminary hypotheses, the results should be considered exploratory. The findings are subject to potential biases, including selection bias, and the

likelihood of chance findings influencing the outcomes is high. Robust validation in a larger, well-characterized cohort is essential before drawing definitive conclusions regarding the genetic landscape of UTUC.

UTUC is a complex disease with a significant impact on patient outcomes. For advanced or metastatic UTUC, chemotherapy is the mainstay of treatment. Commonly used regimens include MVAC (methotrexate, vinblastine, doxorubicin, cisplatin) and gemcitabine-cisplatin combinations. However, the optimal chemotherapy regimen and its long-term benefits are still being explored [17–19]. A comprehensive understanding of its clinical and genetic aspects is essential for improving diagnosis, treatment, and prognosis. Continued research efforts are needed to develop more personalized and effective treatment strategies.

Conclusion

This research investigate the genomic characterization of the UTUC patients using long-read sequencing, including the CNVs, SNVs, SVs, STRs and the methylation levels. The relationship between molecular features and the progression of tumor, prognosis, and sensitivity to medication are valuable to explore. LRS has obvious advantages over NGS in understanding the genomic alterations in somatic cells of tumor tissue, especially in examining structural variations. Therefore, LRS has great application value in understanding the genomic alterations of solid tumors, biomarker discovery, and individualized precision treatment.

Abbreviations

UC	Urothelial carcinoma
UCB	Urothelial carcinoma of the bladder
UTUC	Upper tract urothelial carcinoma
FUSCC	Fudan University Shanghai Cancer Center
MSKCC	Memorial Sloan Kettering Cancer Center
P/LP	Pathogenic/likely pathogenic
SNVs	Single nucleotide variants
NGS	Next-generation sequencing
SVs	Structural variation
LRS	Long-read sequencing
STRs	Short Tandem Repeats
DNAme	DNA methylation
WES	Whole-exome sequencing
WGS	Whole-genome sequencing
CCS	Circular Consensus Sequence
Vep	Variant Effect Predictor
TURBT	Transurethral resection of bladder tumor
GC	Gemcitabine-cisplatin
GP	Gemcitabine-phosphorus
ecDNA	Extrachromosomal DNA
ACMG	American College of Medical Genetics and Genomics
ONT	Oxford Nanopore Technologies
PacBio	Pacific Biosciences

Supplementary Information

The online version contains supplementary material available at https://doi.org/10.1186/s12885-025-15254-x.

Supplementary Material 1: Table S1 Statistics of SNVs detected by WES. Table S2 Sequencing data of WGS by LRS. Table S2 Sequencing data of WGS by LRS. Table S3 Target genes used in screening the results of WGS. Table S4 All SNVs after screening with targeted genes. Table S5 All SVs after screening with targeted genes.

Supplementary Material 2: Figure S1. Aberrant repeat expansions unique to each patient with UTUC.

Supplementary Material 3: Screened SVs identified by WGS.

Acknowledgements

We sincerely thank all the study participants for their involvement in this research. Figure 1A was created with the assistance of BioRender.com.

Authors' contributions

Junlong Wu, Shengming Jin, and Dingwei Ye designed the study; Zhi Shang collected samples; Xiuxin Ling and Zhenhua Cao performed sequencing; Zhi Shang and Xiuxin Ling analyzed the data; Zhi Shang and Xiuxin Ling wrote the manuscript.All authors read and approved the final manuscript.

Funding

We sincerely thank all the study participants for their involvement in this research. This work was supported by the Beijing Xisike Clinical Oncology Research Foundation (Y-Young2023-0087), Shanghai "Rising Stars of Medical Talents" Youth Development Program, and Chinese Urological Cancer Grant (grant number: 011).

Data availability

The data supporting the findings of this study are available with the Accession Number: PRJNA1346317.

Declarations

Ethics approval and consent to participate

The study was approved by the local ethical committee of the Fudan University Shanghai Cancer Center (2008222-22). All patients included have consented to participate in this study. This study was conducted in accordance with the principles of the Declaration of Helsinki. Informed consent was obtained from all participants, and their confidentiality was ensured.

Consent for publication

All authors agree to publish the article.

Competing interests

The authors declare no competing interests.

Author details

[1]Department of Urology, Fudan University Shanghai Cancer Center, No. 270 Dong'an Road, Shanghai 200032, People's Republic of China
[2]Department of Oncology, Shanghai Medical College, Fudan University, Shanghai 200032, China
[3]Shanghai Genitourinary Cancer Institute, Shanghai 200032, China
[4]Bioengineering, Beijing 100080, China

Received: 25 May 2025 / Accepted: 25 October 2025
Published online: 01 December 2025

References

1. Chen X, Wahafu W, Shen Y, Fan J, Yao X. CACA guidelines for holistic integrative management of urothelial carcinoma. Holistic Integrative Oncology. 2024;3(1):9.
2. Colla Ruvolo C, Nocera L, Stolzenbach LF, Wenzel M, Cucchiara V, Tian Z, et al. Incidence and survival rates of contemporary patients with invasive upper tract urothelial carcinoma. Eur Urol Oncol. 2021;4(5):792–801.

3. Roupret M, Babjuk M, Burger M, Capoun O, Cohen D, Comperat EM, et al. European association of urology guidelines on upper urinary tract urothelial carcinoma: 2020 update. Eur Urol. 2021;79(1):62–79.
4. Nassar AH, Umeton R, Kim J, Lundgren K, Harshman L, Van Allen EM, et al. Mutational analysis of 472 urothelial carcinoma across grades and anatomic sites. Clin Cancer Res. 2019;25(8):2458–70.
5. Fujii Y, Sato Y, Suzuki H, Kakiuchi N, Yoshizato T, Lenis AT, et al. Molecular classification and diagnostics of upper urinary tract urothelial carcinoma. Cancer Cell. 2021;39(6):793–809. e8.
6. Shang Z, Pan J, Wang S, Gu C, Zhang H, Shi G, et al. Genomic landscape and clinical relevance in Chinese patients with upper tract urothelial carcinoma. JCO Precis Oncol. 2025;9:e2500195.
7. Roupret M, Babjuk M, Comperat E, Zigeuner R, Sylvester RJ, Burger M, et al. European association of urology guidelines on upper urinary tract urothelial carcinoma: 2017 update. Eur Urol. 2018;73(1):111–22.
8. Carlo MI, Ravichandran V, Srinavasan P, Bandlamudi C, Kemel Y, Ceyhan-Birsoy O, et al. Cancer susceptibility mutations in patients with urothelial malignancies. J Clin Oncol. 2020;38(5):406–14.
9. Nassar AH, Abou Alaiwi S, AlDubayan SH, Moore N, Mouw KW, Kwiatkowski DJ, et al. Prevalence of pathogenic germline cancer risk variants in high-risk urothelial carcinoma. Genet Med. 2020;22(4):709–18.
10. Sfakianos JP, Gul Z, Shariat SF, Matin SF, Daneshmand S, Plimack E, et al. Genetic differences between bladder and upper urinary tract carcinoma: implications for therapy. Eur Urol Oncol. 2021;4(2):170–9.
11. Cosenza MR, Rodriguez-Martin B, Korbel JO. Structural variation in cancer: role, prevalence, and mechanisms. Annu Rev Genomics Hum Genet. 2022;23:123–52.
12. Dubois F, Sidiropoulos N, Weischenfeldt J, Beroukhim R. Structural variations in cancer and the 3D genome. Nat Rev Cancer. 2022;22(9):533–46.
13. Ardui S, Ameur A, Vermeesch JR, Hestand MS. Single molecule real-time (SMRT) sequencing comes of age: applications and utilities for medical diagnostics. Nucleic Acids Res. 2018;46(5):2159–68.
14. Rausch T, Snajder R, Leger A, Simovic M, Giurgiu M, Villacorta L, et al. Long-read sequencing of diagnosis and post-therapy Medulloblastoma reveals complex rearrangement patterns and epigenetic signatures. Cell Genom. 2023;3(4):100281.
15. Conlin LK, Aref-Eshghi E, McEldrew DA, Luo M, Rajagopalan R. Long-read sequencing for molecular diagnostics in constitutional genetic disorders. Hum Mutat. 2022;43(11):1531–44.
16. Wu J, Jin S, Gu C, Wei Y, Zhu Y, Necchi A, et al. Inherited mutations in Chinese patients with upper tract urothelial carcinoma. Cell Rep Med. 2023;4(1):100883.
17. Margulis V, Shariat SF, Matin SF, Kamat AM, Zigeuner R, Kikuchi E, et al. Outcomes of radical nephroureterectomy: a series from the upper tract urothelial carcinoma collaboration. Cancer. 2009;115(6):1224–33.
18. Pierconti F, Martini M, Fiorentino V, Cenci T, Racioppi M, Foschi N, et al. Upper urothelial tract high-grade carcinoma: comparison of urine cytology and DNA methylation analysis in urinary samples. Hum Pathol. 2021;118:42–8.
19. Sanford T, Porten S, Meng MV. Molecular analysis of upper tract and bladder urothelial carcinoma: results from a microarray comparison. PLoS ONE. 2015;10(8):e0137141.
20. Guo G, Sun X, Chen C, Wu S, Huang P, Li Z, et al. Whole-genome and whole-exome sequencing of bladder cancer identifies frequent alterations in genes involved in sister chromatid cohesion and segregation. Nat Genet. 2013;45(12):1459–63.
21. Hurst CD, Alder O, Platt FM, Droop A, Stead LF, Burns JE, et al. Genomic subtypes of Non-invasive bladder cancer with distinct metabolic profile and female gender bias in KDM6A mutation frequency. Cancer Cell. 2017;32(5):701–15. e7.
22. Pietzak EJ, Bagrodia A, Cha EK, Drill EN, Iyer G, Isharwal S, et al. Next-generation sequencing of nonmuscle invasive bladder cancer reveals potential biomarkers and rational therapeutic targets. Eur Urol. 2017;72(6):952–9.
23. Robertson AG, Kim J, Al-Ahmadie H, Bellmunt J, Guo G, Cherniack AD, et al. Comprehensive molecular characterization of Muscle-Invasive bladder cancer. Cell. 2017;171(3):540–56. e25.
24. Loriot Y, Kamal M, Syx L, Nicolle R, Dupain C, Menssouri N, et al. The genomic and transcriptomic landscape of metastatic urothelial cancer. Nat Commun. 2024;15(1):8603.
25. Kluth M, Hitzschke M, Furlano K, Plage H, Hofbauer S, Weinberger S. 17p13 (TP53) deletions are associated with an aggressive phenotype but unrelated to patient prognosis in urothelial bladder carcinomas. Genes Chromosomes Cancer. 2024;63(9):e23271.
26. Nguyen DD, Hooper WF, Liu W, Chu TR, Geiger H, Shelton JM, et al. The interplay of mutagenesis and ecdna shapes urothelial cancer evolution. Nature. 2024;635(8037):219–28.
27. Guardiola MT, Dobin SM, Dal Cin P, Donner LR. Pericentric inversion (12)(p12q13-14) as the sole chromosomal abnormality in a leiomyoma of the vulva. Cancer Genet Cytogenet. 2010;199(1):21–3.
28. Welborn J, Jenks H, Taplett J, Walling P. Inversion of chromosome 12 and lineage promiscuity in hematologic malignancies. Cancer Genet Cytogenet. 2004;148(2):91–103.
29. Uehara S, Tanigawara S, Takeyama Y, Okamura K, Yajima A. A family with pericentric inversion of chromosome 12. Jpn J Hum Genet. 1994;39(1):201–4.
30. Klein U, Lia M, Crespo M, Siegel R, Shen Q, Mo T, et al. The DLEU2/miR-15a/16 – 1 cluster controls B cell proliferation and its deletion leads to chronic lymphocytic leukemia. Cancer Cell. 2010;17(1):28–40.
31. Khalid K, Padda J, Syam M, Moosa A, Kakani V, Sanka S, et al. 13q14 deletion and its effect on prognosis of chronic lymphocytic leukemia. Cureus. 2021;13(8):e16839.
32. Zenz T, Eichhorst B, Busch R, Denzel T, Habe S, Winkler D, et al. TP53 mutation and survival in chronic lymphocytic leukemia. J Clin Oncol. 2010;28(29):4473–9.
33. Rouault A, Banneau G, Macgrogan G, Jones N, Elarouci N, Barouk-Simonet E, et al. Deletion of chromosomes 13q and 14q is a common feature of tumors with BRCA2 mutations. PLoS ONE. 2012;7(12):e52079.
34. Robinson TJ, Liu JC, Vizeacoumar F, Sun T, Maclean N, Egan SE, et al. RB1 status in triple negative breast cancer cells dictates response to radiation treatment and selective therapeutic drugs. PLoS ONE. 2013;8(11):e78641.
35. Erwin GS, Gursoy G, Al-Abri R, Suriyaprakash A, Dolzhenko E, Zhu K, et al. Recurrent repeat expansions in human cancer genomes. Nature. 2023;613(7942):96–102.
36. Bui C, Huber C, Tuysuz B, Alanay Y, Bole-Feysot C, Leroy JG, et al. XYLT1 mutations in desbuquois dysplasia type 2. Am J Hum Genet. 2014;94(3):405–14.
37. Van Daele SH, Moisse M, van Vugt J, Zwamborn RAJ, van der Spek R, van Rheenen W, et al. Genetic variability in sporadic amyotrophic lateral sclerosis. Brain. 2023;146(9):3760–9.
38. Tazelaar GHP, Dekker AM, van Vugt J, van der Spek RA, Westeneng HJ, Kool L, et al. Association of NIPA1 repeat expansions with amyotrophic lateral sclerosis in a large international cohort. Neurobiol Aging. 2019;74:234. e9- e15.
39. Kuo YJ, Lewis JS Jr., Zhai C, Chen YA, Chernock RD, Hsieh MS, et al. DEK-AFF2 fusion-associated papillary squamous cell carcinoma of the sinonasal tract: clinicopathologic characterization of seven cases with deceptively bland morphology. Mod Pathol. 2021;34(10):1820–30.

Publisher's Note